Numerical Simulation of Two-Phase Fluid-Structure Interaction in Fractured Formation Under Drilling Conditions

Yige Zhao[1], Zhiyuan Wang[1,2(✉)], Hongzhi Xu[3], Jiayi Shen[1], Jianbo Zhang[1,2], and Hui Liu[1]

[1] School of Petroleum Engineering, China University of Petroleum (East China), Qingdao 266580, China
`wangzy1209@126.com`
[2] National Engineering Research Center of Oil and Gas Drilling and Completion Technology, Qingdao, Shandong, People's Republic of China
[3] CNPC Offshore Engineering Company Limited, Beijing 100282, China

Abstract. In the course of drilling fractured formation, influenced by drilling parameters and different working conditions, the stress distribution around the well changes, resulting in fracture opening or closing, easy to cause leakage or overflow and other well control accidents. In this study, COMSOL Multiphysics software is used to simulate the stress variation, fracture deformation and gas-liquid two-phase saturation distribution around a well under different drilling conditions and fracture patterns. It is found that the fractures will open in different degrees when drilling vertical and parallel to the wellbore, and the crack opening and permeability will increase gradually with time, the distribution of near-well zone fluid saturation becomes wider, which shows that the drilling fluid gradually invades the fracture with the opening of the fracture and bursts into the depth of the formation Under the action of exciting pressure, fracture width and permeability are larger than those under normal drilling, The two-phase fluid-solid coupling law of fractured formation obtained in this study provides a reference for field well control program.

Keywords: drilling condition · fractured formation · fluid-structure interaction · COMSOL Multiphysics · well control

1   Introduction

When drilling fractured formation, the stress distribution around the well is changed under the influence of construction parameters and different working conditions, which leads to the opening or closing of the fracture and changes the conductivity of the fracture. Studying the fluid-solid coupling mechanism of fractures in wellbore working environment, designing and calculating the change of fracture shape and the distribution of stress field around the wellbore under different operating parameters and working conditions when over-balanced drilling, and influenced by the change of bottom-hole pressure, the

change law of seepage ability of fractured formation. Evans et al. put forward a log model of normal deformation of fractures, but this model is not suitable for high stress formation conditions [1]. Goodman et al. explained the mechanics mechanism of normal deformation of crack, and proved the nonlinear law of crack closure similar to hyperbolic when normal stress increased [2]. Based on this, Bandis and Barton have carried out experiments on a large number of rock samples containing unfilled natural fractures, and put forward a hyperbolic model of normal deformation of fractures, the model can be used to describe the closing mechanism of natural fractures in fractured reservoirs [3]. Bai et al. first considered the effect of medium deformation on fracture permeability in flow simulation [4], Bagheri and Settari incorporated the effect of fracture deformation into the dual medium model by coupling stress tensor and fracture permeability [5], but in the early numerical simulation research, the crack treatment technology is not mature enough.

Using COMSOL Multiphysics, the stress variation around a well, the seepage law of fracture deformation and the distribution of gas-liquid two-phase saturation under different drilling conditions and fracture patterns are simulated.

2   Numerical Simulation

2.1   Governing Equation

The mass conservation equations of water and gas in porous media are:

$$\frac{\partial(\varphi \rho_w s_w)}{\partial t} - \nabla \cdot (K \rho_w \lambda_w \nabla p_w) = m_w \tag{1}$$

$$\frac{\partial(\varphi \rho_g s_g)}{\partial t} - \nabla \cdot (K \rho_g \lambda_{rg} \nabla p_g) = m_g \tag{2}$$

$$s_w + s_g = 1 \tag{3}$$

where φ is the total porosity of the naturally fractured shale matrix. λ_{rw} is the relative mobility of water, and $\lambda_{rw} = k_{rw}/\mu_w$. K is the permeability matrix. p_w and S_w are respectively the pressure and saturation of water phase. p_g and s_g are respectively the pressure and saturation of gas phase. λ_{rg} is the relative mobility of gas, and $\lambda_{rg} = k_{rg}/\mu_g$. K_{rg} is the apparent permeability of gas phase when we consider different flow mechanisms. ρ_w and ρ_g are respectively the water density and gas density. m_w and m_g are respectively mass sources of water and gas.

Considering the water and rock as slightly compressible material, thus we have:

$$\rho_w = \rho_w^{ini} e^{c_w(p_w - p^{ini})} = \rho_w^{ini}[1 + c_w(p_w - p^{ini})] \tag{4}$$

$$\varphi = \varphi^{ini} e^{c_p(p_w - p^{ini})} = \varphi^{ini}\left[1 + c_p\left(p_w - p^{ini}\right)\right] \tag{5}$$

where c_p is the pore compressibility coefficient the superscript -ini means the initial state.

With Eq. (4) and Eq. (5), the time derivative and convection terms of Eq. (1) can be expressed as:

$$\frac{\partial(\varphi\rho_w S_w)}{\partial t} = \rho_w^{ini}\varphi^{ini}c_{tw}S_w\frac{\partial p_w}{\partial t} + \rho_w\varphi\frac{\partial S_w}{\partial t} \tag{6}$$

$$\nabla\cdot(K\rho_w\lambda_{rw}\nabla p_w) = K\nabla\cdot\left(\lambda_{rw}\rho_w^{ini}e^{c_w(p_w-p^{ini})}\nabla p_w\right) = K\nabla\cdot\left(\lambda_{rw}\rho_w^{ini}\nabla\frac{e^{c_w(p_w-p^{ini})}}{c_w}\right)$$

$$= K\rho_w^{ini}\left[\frac{d\lambda_{rw}}{ds_s}\nabla s_w\cdot\nabla p_w + \lambda_{rw}\nabla^2 p_w\right] = K\rho_w^{ini}\lambda_{rw}\nabla^2 p_w \tag{7}$$

where $c_{tw} = c_w + c_p$. In Eq. (6), we neglect the quadratic infinitesimals containing $c_p c_w$. In Eq. (7), $\nabla S_w\cdot\nabla p_w$ and $\nabla p_w\cdot\nabla p_w$ are also neglected.

Substitute Eq. (6) and Eq. (7) into Eq. (1), we get the flow equation of the slightly compressible water in the slightly compressible porous media.

$$\rho_w^{ini}\varphi^{ini}c_w S_w\frac{\partial p_w}{\partial t} + \rho_w\varphi\frac{\partial S_w}{\partial t} - K\rho_w^{ini}\lambda_w\nabla^2 p_w = m_w \tag{8}$$

Divide ρ_w^{ini} on both sides of the equation at the same time. Compared with the time derivative of the pressure, the time derivative of the water saturation is an infinitesimal. Thus, we get:

$$\varphi^{ini}c_{tw}s_w\frac{\partial p_w}{\partial t} + \varphi\frac{\partial s_w}{\partial t} - K\lambda_{rw}\nabla^2 p_w = q_w \tag{9}$$

where $q_w = m_w/\rho_w^{ini}$.

The state equation of ideal gas is:

$$\rho_g = \frac{p_g M}{RT} \tag{10}$$

Then we have the following relation:

$$\rho_g = \rho_g^{ini}\frac{p}{p^{ini}} \tag{11}$$

With Eq. (10) and Eq. (11), the time derivative term of Eq. (2) can be expressed as:

$$\frac{\partial(\varphi\rho_g s_g)}{\partial t} = \left(\varphi\frac{\rho_g^{ini}}{p_g^{ini}} + \varphi^{ini}c_p p_g\right)s_g\frac{\partial p_w}{\partial t} + \varphi\rho_g\frac{\partial s_g}{\partial t} \tag{12}$$

Then we obtain the gas flow equation:

$$\varphi^{ini}c_{tg}s_g\frac{\partial p_w}{\partial t} + \varphi\frac{\partial s_g}{\partial t} - K\lambda_{rg}\left(\nabla^2 p_w + \frac{dp_c}{ds_w}\nabla^2 s_w\right) = q_g \tag{13}$$

By adding Eq. (9) and Eq. (13), we can get the following equation and it can be assembled into the matrix form:

$$\begin{bmatrix}\varphi^{ini}(c_{iq}s_s + c_{no}s_w) & 0 \\ \varphi^{im}c_{tw}s_w & \varphi\end{bmatrix}\begin{pmatrix}\dot{p}_w \\ \dot{s}_w\end{pmatrix} + \begin{bmatrix}-K\lambda_t & K\lambda_s\frac{dp_{c-m}}{ds_w} \\ -K\lambda_{rw} & 0\end{bmatrix}\begin{pmatrix}\nabla^2 p_w \\ \nabla^2 s_w\end{pmatrix} = \begin{pmatrix}q_{s-m} + q_{v-m} \\ q_{v-m}\end{pmatrix} \tag{14}$$

2.2 Modeling and Boundary Conditions

The geometric model is shown in Fig. 1. Two sets of fractures are set, one is two high angle fractures passing through the wellbore, the other is inclined fractures crossing each other. Set the observation point at the connection point. 1 is 1/4 wellbore, the diameter of wellbore is 20 cm, the constant pressure boundary is 102 MPa and the initial formation pressure is 98 MPa. Using free triangle mesh, the number of cells is 4026, the minimum cell mass is 0.5259, the average cell mass is 0.9053.
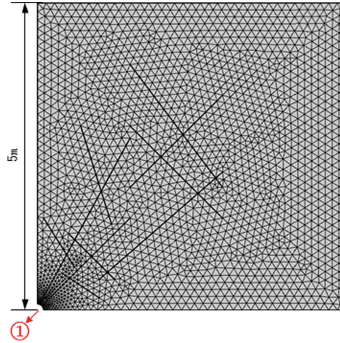
Fig. 1. Geometric models and meshing

3   Results and Analysis

3.1 Saturation and Pressure

Figures 2 and 3 show A cloud of saturation and pressure changes over 1000 min.

| (a)0min | (b)200min | (c)400min |

| (d)600min | (e)800min | (f)1000min |
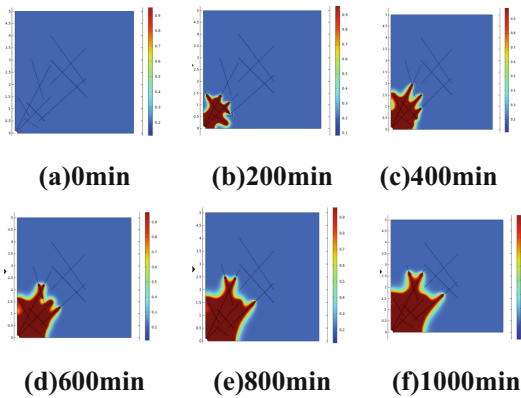
Fig. 2. Clouds of saturation changes over 1000 min.
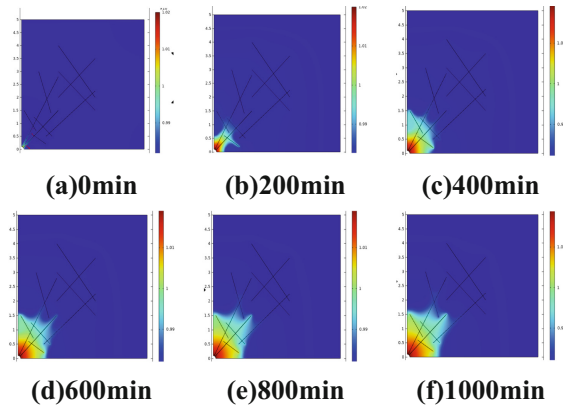
Fig. 3. Clouds of pressure changes over 1000 min.

With the opening of the fracture, drilling fluid gradually invades the fracture and formation, and erupts to the depth of formation. The pressure propagation is non-uniform, and the pressure near the wellbore is larger and the pressure propagation is faster in the fractures connecting the wellbore.

3.2 Different Drilling Parameters

In drilling engineering, it is over-balanced drilling when the effective pressure of the drilling fluid string is greater than the formation pressure, when the drilling fluid pressure is greater than the formation fluid pressure and less than the formation fracture pressure, drilling fluid will invade some of the formation, and can effectively inhibit formation fluid into the wellbore, prevent overflow blowout and other accidents, to ensure the safety of drilling wellhead. According to the bottom hole pressure calculated at 6782.3 m, the bottom hole pressure is 102 MPa and the original formation pressure is 98 MPa, and the results were compared with the results of excited pressure and suction pressure. Figure 4 shows the change of connecting wellbore fracture opening under over-balanced drilling; Fig. 5 shows the change of permeability of connected wellbore fractures under over-balanced drilling; Fig. 6 shows the change of leakage rate under over-balanced drilling conditions; Fig. 6 shows the change of Cumulative amount of leakage under over-balanced drilling conditions.

From Figs. 4 and 5, it can be seen that the fractures will open in different degrees when drilling through high-angle connected wellbore fractures. Under the action of exciting pressure, fracture width and permeability are larger than those under normal drilling, while under the action of suction pressure, fracture width and permeability are smaller than those under normal drilling. From Figs. 6 and 7, it can be seen that the leakage rate changes greatly in the process of pressure propagation in the fracture, and the leakage rate in the fracture is larger in the initial stage, after the pressure transmission is over, when the pressure in the fracture is redistributed, the leakage rate in the fracture decreases rapidly, and the leakage rate in the later period decreases slowly, however,
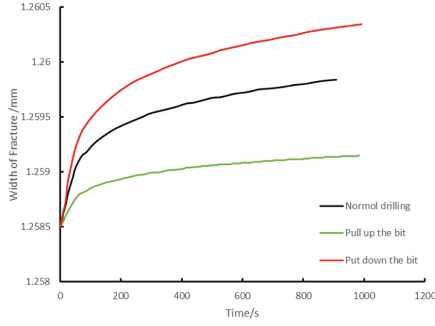
Fig. 4. The change of connecting wellbore fracture opening under over-balanced drilling in 1000 s
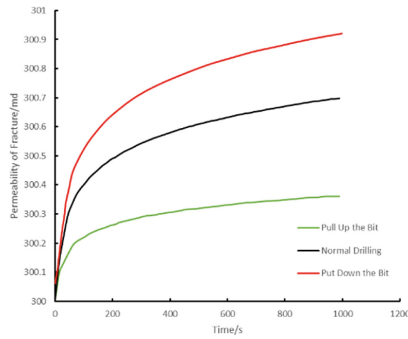
Fig. 5. The change of connecting wellbore fracture permeability under over-balanced drilling in 1000 s
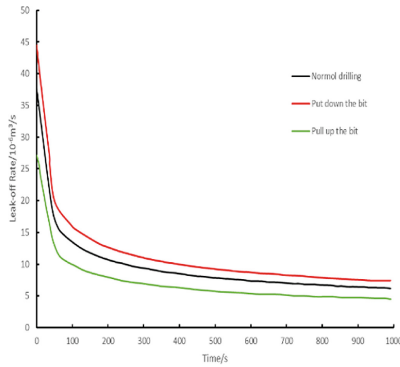
Fig. 6. The change of leakage rate under over-balanced drilling conditions in 1000 s

under the influence of suction pressure, the loss will be smaller than that in normal drilling, and the cumulative loss will increase with time and increase nonlinearly.
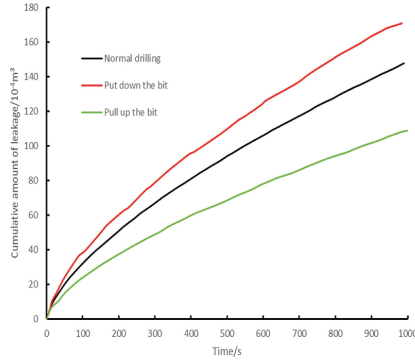
Fig. 7. The change of Cumulative amount of leakage under over-balanced drilling conditions in 1000 s

4   Conclusion

By using COMSOL Multiphysics software, the stress variation, fracture deformation and gas-liquid two-phase saturation distribution around a well under different drilling conditions and fracture patterns are simulated, the following conclusions were reached:

When high-angle connected wellbore fractures are drilled by over-balanced drilling, the fractures will open in different degrees. Under the action of exciting pressure, fracture width and permeability are larger than those under normal drilling, while under the action of suction pressure, fracture width and permeability are smaller than those under normal drilling.

In the process of pressure propagation in the fracture, the leakage rate changes greatly, and the leakage rate in the initial stage of the fracture is large, the rate of leakage in the fracture decreases rapidly, and the rate of leakage in the later period decreases slowly, however, under the influence of suction pressure, the loss will be smaller than that in normal drilling, and the cumulative loss will increase with time and increase nonlinearly.

References

1. Goodman, R.E.: Petroleum reservoir simulation coupling fluid flow and geomechanics. SPE Reservoir Eval. Eng. **4**(3), 164–172 (1974)
2. Bandis, S.C., Lumsden, A.C., Barton, N.R.: Fundamentals of rock joint deformation. Int. J. Rock Mech. Min. Sci. Geomech. **20**(6), 249–268 (1984)
3. Barton, N.R., Bandis, S.C., Bakhtar, K.: Strength, deformation and conductivity coupling of rock joints. Int. J. Rock Mech. Min. Sci. Geomech. **22**(3), 121–140 (1985)

4. Bai, M., Meng, F., Elsworth, D., et al.: Numerical modeling of coupled flow and deformation in fractured rock specimens. Int. J. Numer. Analyt. Meth. Geomech. **23**, 141–160 (1999)
5. Bagheri, M., Settari, A.: Modeling of geomechanics in naturally fractured reservoirs. SPE Reservoir Eval. Eng. **11**(1), 108–118 (2008)